Journal of Geomatics Vol 8 No. 2 October 2014

Building subsidence estimation using PSInSAR technique: Case study of Mumbai city

Shweta Sharma*, Y.S. Rao^ and Ajai*
*Space Applications Centre, ISRO, Ahmedabad
^IIT Bombay, Mumbai
Email: shweta@sac.isro.gov.in

(Received: Aug 05, 2014; in final form: Sep 25, 2014)

Abstract: This study aims to map and monitor land displacement over the Mumbai city and surroundings using Persistent Scatterer Interferometry Synthetic Aperture Radar (PSInSAR) technique. As Mumbai city comprises of many natural reflectors that work as a stable radar target, PS Interferometry technique has been utilized in the study. For the first time, the land deformation mapping of Mumbai city and surroundings has been done using Persistent Scatterer Interferometry (PSI) technique and attempt was made to estimate the building subsidence. ENVISAT and ERS-1/2 data were acquired over Mumbai through European Space Agency (ESA) Cat-1 project and data were processed using PSInSAR method and displacement map was generated. From the qualitative analysis of displacement map and identification of the building PS points, it was found that the buildings in Mumbai city are undergoing subsidence at the mean velocity of 5mm/year. The displacement velocity map generated by processing of ERS and ENVISAT combined data was divided into high, medium and low subsidence area due to the non-availability of field data for validation. The cause of the subsidence might be attributed to the lowering of ground water level, hydrogeology, construction in marshy land, weak soil, weight of buildings, etc. of the area.

Keywords: SAR, PSInSAR, Building subsidence, Stable scatterers, Land deformation map

1. Introduction

Urban ground motion due to natural or man-made geological processes is an issue of major importance for local authorities, property developers, planners, residents of the area and buyers. There is an urgent need to gain knowledge about this phenomenon as it would benefit all involved. Due to the urbanization, many cities are facing building sinking problem. Because of the improper foundation, compaction of overlying confining layer material takes place which results in sinking of the buildings. This land deformation phenomenon is slow in nature and therefore long time period data is needed i.e. data for several years is required for the study area for proper modeling of the land deformation process. However, long time period may give rise to temporal decorrelation and loss of coherence may occur which limits the application of conventional interferometry technique for this type of study.

Numerous studies have been done to study land deformation using differential interferometry approach. Differential interferometry uses the phase difference between two radar images (2-pass) taken at two different times and an external digital elevation model (DEM) or three (3-pass) or four radar images (4-pass) taken at different appropriate dates to provide a measure of the ground movement with sub-centimeter accuracy. Because of the several limitations (temporal decorrelation, spatial decorrelation etc.) of the conventional differential interferometry technique, advanced differential interferometry techniques like PSInSAR (Ferretti et al., 2001), Small Baseline Subset (SBAS) technique (Berardino et al., 2002) and very recently SqueeSAR algorithm (Ferretti et al., 2011) have been developed. SqueeSAR algorithm is useful for the rural areas where not much stable scatterers are found. Globally, work has been initiated to study the building and infrastructure deformation (Cascini et al. 2013; Yonghong et al., 2014; Crosetto et al., 2013, 2014). Karila et al. (2013) used PSInSAR technique for building subsidence study and compared the results with the levelling data. They found the building subsidence values in the range -12.2 to 12.15 mm/year. In India, first time building subsidence study using satellite SAR Interferometry is being attempted.

For land deformation study in city area, PSInSAR is useful technique as city comprises of many natural reflectors that work as a stable radar target. Persistent scatterers are radar targets that have coherent phase behavior over a long period of time (mostly man-made features in the terrain). The phase difference observations from these targets are used for estimating the deformation signal and atmospheric disturbances. They form a network of points where measurements are reliable and in which phase unwrapping can be performed. PS Technique has been successfully applied in urbanized areas where PS density is high. As Mumbai city comprises of many natural reflectors that work as a stable radar target, PS Interferometry technique has been utilized in this study.

The knowledge of urban ground deformation and its underlying causes will be very helpful to the residents, insurance companies and property buyers. Damage to buildings and infrastructure can seriously injure and endanger the lives of the people, also it costs insurance companies a huge loss. The information that will alert the people before such type of damage actually take place is therefore invaluable.

2. Objective of the study

This study aims to map land displacement and identification of endangered buildings in the Mumbai city. For urbanization, wet lands and agricultural lands are being converted for constructing multi-storey buildings in Mumbai. Because of the improper foundation, compaction of overlying confining layer material takes place which results in sinking of the buildings. The information on PS points has been utilized to obtain land deformation map for the study area.

3. Study area and data used

In order to map the endangered buildings due to land subsidence, a part of Mumbai city and surroundings (shown in Fig.1) has been selected. Since the city is located at coastal area and because of urbanization and migration of people from all other states to Mumbai for better lifestyle, more land is needed for construction purposes. Hence, in Mumbai, wet lands and agricultural lands are being converted for constructing multi storied buildings. The buildings that are constructed on such improper foundation may subside slowly and eventually may fall over a long period of time. So, it is very important to map such endangered buildings in order to prevent the disaster from happening. This land deformation phenomenon is slow in nature and long time period data is needed i.e. data for several years is required for the study area for proper modeling of the land deformation event. Because of the above said reasons and owing to the fact that nobody has attempted such type of study till date for Mumbai city, Mumbai city and surroundings has been chosen as the study area. The mean intensity image of the study area is shown in Fig. 1.

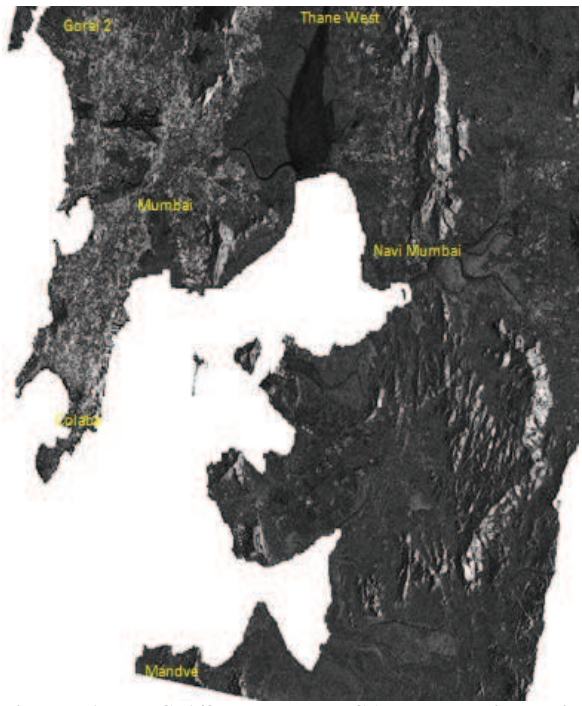

Figure 1: ERS-1/2 and ENVISAT mean intensity image of the study area

The data used in the present study is of ERS-1/2 and ENVISAT data. The data was acquired through the ESA Cat-1 project (project ID: 14600). ENVISAT beam 'IS2' having swath 103.94 km with VV polarization has been used in the study. Other than ENVISAT IS2 beam, we cannot combine data with ERS-1/2. Azimuth spacing and range spacing for ENVISAT is 4.05 m and 7.8 m respectively whereas, ERS data has line spacing of 3.9 m and pixel spacing of 7.904 m. 16 images of ERS and ENVISAT were processed to generate the land deformation map. As the processing takes long time, only a small part of full scene is processed. For identification of the building points, IRS-P6 Liss-4 image (spatial resolution 5.8 m) with Segment no. 2, Strip No. 2 and Scene No. 113 of 16th February 2008 was used. Table 1 shows the description of the microwave data (ERS and ENVISAT data with corresponding baseline values) used in the study.

Table 1: ERS-1/2 and ENVISAT data description

S. No.	Satellite	Date of Acquisition	Perpendicular Baseline (m)
1	ERS 1	28-May-1992	0
2	ERS 1	24-Dec-1992	-556.885
3	ERS 1	04-Mar-1993	-164.822
4	ERS 1	08-Apr-1993	398.795
5	ERS 1	20-Apr-1996	925.034
6	ERS 1	25-May-1996	-126.569
7	ERS 2	26-May-1996	-245.817
8	ERS 2	07-Dec-1997	-122.386
9	ERS 2	16-May-1999	375.192
10	ERS 2	20-Jun-1999	-227.715
11	ERS 2	18-Jul-2004	-164.688
12	Envisat	16-Nov-2003	-826.247
13	Envisat	04-Apr-2004	741.624
14	Envisat	31-Oct-2004	460.863
15	Envisat	20-Mar-2005	-376.347
16	Envisat	27-Jun-2010	-79.252

4. Methodology

In this work, Persistent Scatterer interferometry technique (PSInSAR) has been used. The flowchart of the steps involved in the technique is shown in Figure 2. As shown in flowchart, input to PSI process is a stack of differential interferograms coregistered to a selected master interferogram. The master image is selected based on the stack coherence (Kampes and Nico, 2005). The stack coherence is a function of perpendicular baseline $B_\perp$, temporal baseline T and Doppler centroid frequency f_{dc} and is given in Eq. (1).

$$\gamma^m = \frac{1}{K}\sum_{k=1}^{K} g(B_\perp^{k,m}, B_{\perp_{max}}) \cdot g(T^{k,m}, T_{max}) \cdot g(f_{dc}^{k,m}, f_{dc_{max}}), \quad (1)$$

$$g(x,c) = \begin{cases} 1 - |x|/c & \text{for } |x| \le c, \\ 0 & \text{for } |x| > c, \end{cases}$$

where 'm' refers to the master acquisition and 'K' to the total number of slave acquisitions; $B_{\perp_{max}}$, T_{max} and

f_{dcmax} are the critical value of perpendicular baseline, time span of the images used and critical value of the azimuth bandwidth, respectively.

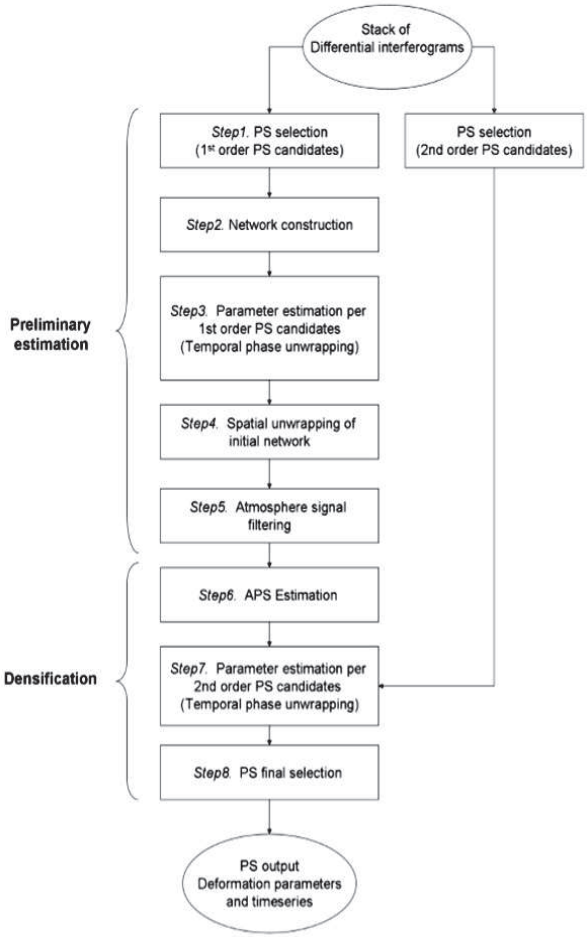

Figure 2: Flowchart showing steps involved in PSInSAR (Source: Esfahany, 2008)

In this study, 28 May 1992 was selected as the master image. The normal baselines corresponding to this master image have been given in table 1. In order to remove the topography related fringes, SRTM DEM was used and differential interferograms were generated. The step is necessary to eliminate the topography related fringes. After the differential interferogram generation step, Persistent scatterers i.e. radar stable targets were selected based on the coherence threshold value. The coherence threshold value of 0.80 was used in this study as lower PS density values (500 and 7 final PS points corresponding to coherence threshold of 0.85 and 0.90 respectively) were obtained for higher coherence threshold values. Since the analysis is done only on the selected PS points, this step is the key step in PSInSAR technique. This step should be performed with great care as the accuracy of the selected PS points will determine the accuracy of the displacement map generated. The required PS density is strongly dependent upon the SAR system spatial resolution, wavelength and revisiting cycle. Number of final PS points obtained for 0.80 coherence threshold value was 71,100 for an area of 40*40 km^2.

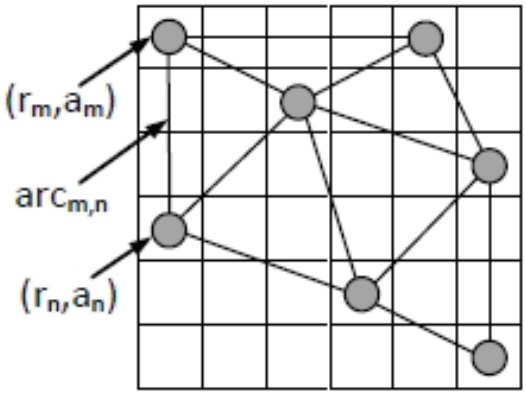

Figure 3: Diagram showing the grey dots as the selected pixels, linked by arcs, generating a grid of non-overlapped triangles

After selection of the PS points, they were joined by the network of arcs as shown in Fig.3. The distance between the two PS points in an arc is chosen in such a way so as to minimize atmospheric error. The phase difference between the mth and nth PS points contains the contributions from following components (Ketelaar, 2009):

$$\Delta\phi = \frac{4\pi}{\lambda} \cdot T_i \cdot (v_m - v_n) + \frac{4\pi}{\lambda} \frac{B_i}{r_0 \cdot \sin\theta_i} (\varepsilon_m - \varepsilon_n) + (\beta_m - \beta_n) + (\eta_m - \eta_n) + (n_m - n_n) \quad (2)$$

Where λ is the wavelength, T_i and B_i are the temporal and spatial baselines for the i^{th} interferogram, v_m, v_n are the linear deformation rates at 'm' and 'n' PS points, ε_m, εn are the topographic errors, β_m, βn are the non-linear deformation components and n_m, n_n account for all noise. After the formation of a network and calculation of relative phase observation per arc, the phases are unwrapped per arc in time together with the estimation of the parameter of interests. The basic task is to estimate the parameter of interest (e.g., relative deformation rate, residual height difference, etc.) and integer ambiguities from wrapped phase values. For temporal unwrapping, 'ambiguity function' method has been used. Spatial unwrapping was carried out simply by path integration of temporally unwrapped phases without residues. However, in practice, non-zero residues are found at the arcs of the network, due to incorrect relative estimations at certain arcs due to noise in the observations. So, the unwrapping errors were detected and corrected. Once the unwrapped phases are obtained per 1st order PS, atmospheric delay phases can be filtered.The atmosphere phase screen is estimated based on the fact that the atmosphere is spatially correlated but temporally uncorrelated. So, by applying low pass filter in the spatial domain and high pass filter in the temporal domain, the atmospheric signals were filtered out. After subtracting the atmospheric phase and refining the network arcs, parameters are once again calculated. For final PS, the topographic height (i.e., subtracted topography plus estimated height residual), deformation parameters, atmospheric phase, and residual phase (assumed to represent unmodeled

deformation) were calculated relative to a single reference point.

5. Results and discussions

The land deformation velocity map generated using ERS and ENVISAT images for a small area of Mumbai city and surroundings and corresponding precision values i.e. mean velocity error in mm/year are shown in Fig.4a and 4b respectively. It is evident from the statistics that the area is experiencing deformation with the rate in the range of -39±0.09 mm/year to 9±0.23 mm/year with mean velocity error of ±0.14mm/year as shown in Fig.4b. The subsidence is divided into high, medium and low (Fig. 4a). This is done due to the non-availability of field data for validation.

The deformation velocity in mm/year with the displacement value in mm at every date with respect to the master image (28th May 1992) for seven random PS points are shown in table 2. From the table it is clear that these PS points are undergoing subsidence and they come under the category of low subsidence.

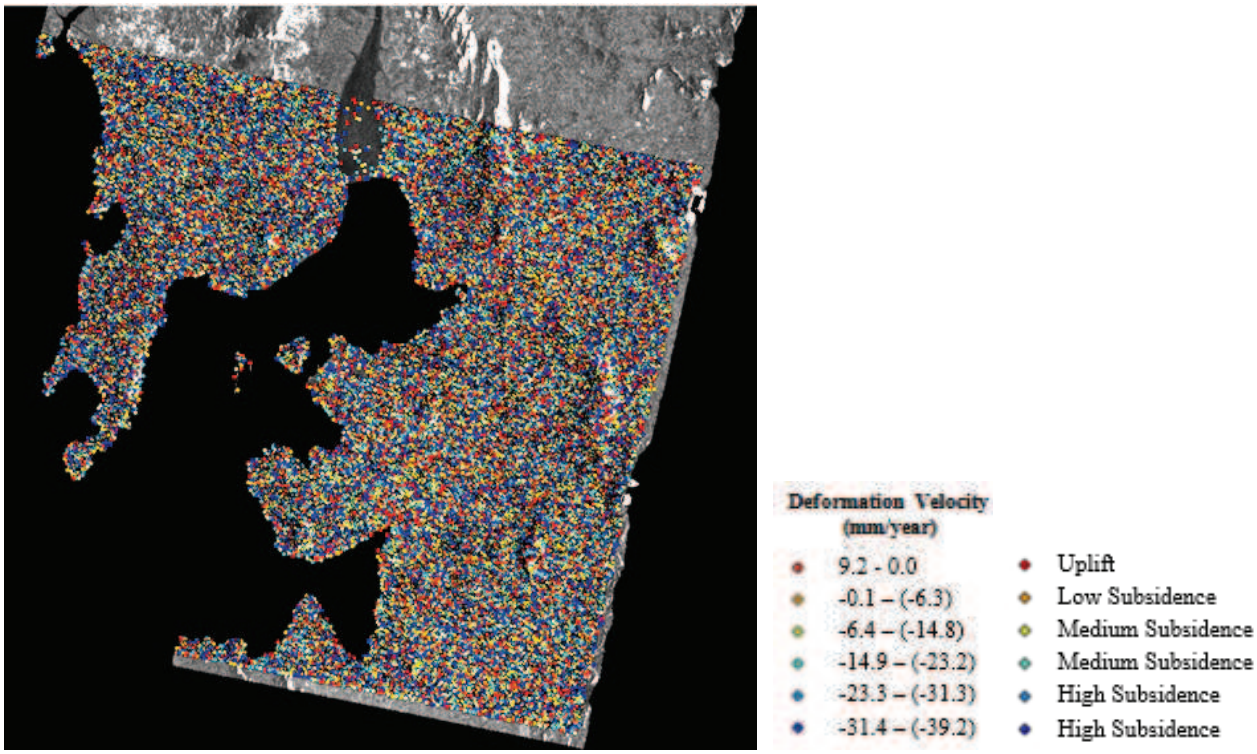

Figure 4(a): Land deformation velocity map (superimposed on mean intensity image) generated for Mumbai city and surroundings

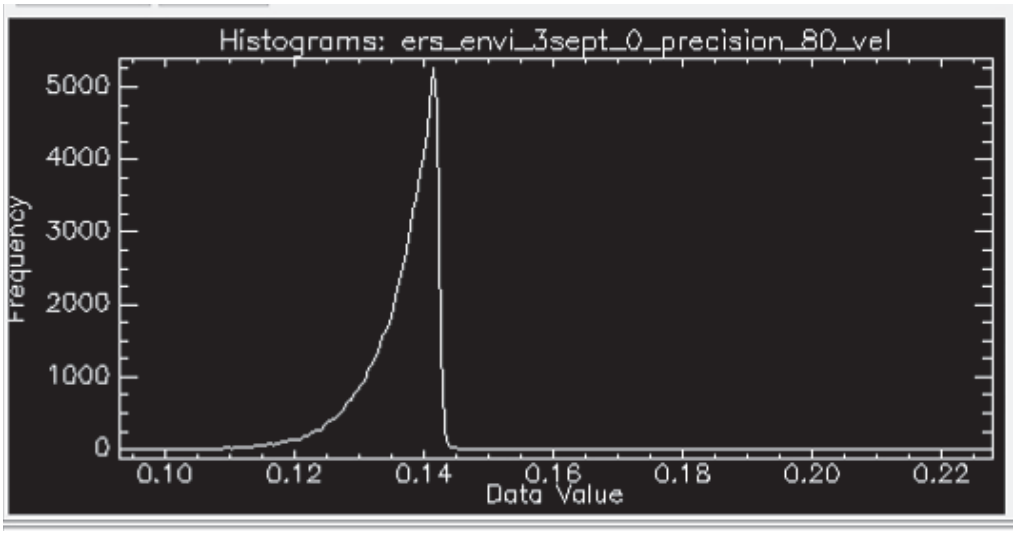

Figure 4(b): Histogram of the precision values (mean velocity error in mm/year)

Table 2: Mean deformation velocity (in mm/year) and displacement value in mm for each date with respect to master date for seven random PS points

S. No.	1	2	3	4	5	6	7
Longitude (E)	**73.0575**	**72.8896**	**73.0029**	**73.1477**	**73.0205**	**73.1236**	**72.8650**
Latitude (N)	**18.9980**	**19.0591**	**18.9228**	**19.0515**	**19.0391**	**18.9384**	**19.0415**
Mean Velocity (mm/year)	-3.9923	-4.0553	-3.9251	-3.9871	-3.9121	-4.1165	-4.1712
D_19920528	0.0000	0.0000	0.0000	0.0000	0.0000	0.0000	0.0000
D_19921224	-7.4875	-7.6774	-0.3949	-5.2486	-6.1125	2.8916	4.3965
D_19930304	-8.9200	-5.6978	-3.2900	-5.4942	-10.2068	-3.6315	-2.5788
D_19930408	-9.9100	-11.1414	-7.7381	-11.8374	-12.2580	-8.0581	-4.6490
D_19960420	-16.9770	-10.9273	-3.3191	-13.0425	-13.3574	-2.9819	-4.2197
D_19960525	-17.0321	-13.4951	-12.2846	-14.4096	-13.4881	-7.5563	-5.1740
D_19960526	-15.9398	-17.1501	-11.2071	-19.6444	-22.1674	-7.3471	-8.5084
D_19971207	-18.4509	-16.4993	-9.8437	-13.4068	-17.5712	-14.9330	-34.0863
D_19990516	-24.4119	-18.0484	-35.7910	-18.2375	-14.8661	-35.9903	-37.5846
D_19990620	-15.8524	-19.3927	-40.1477	-41.5743	-17.3425	-38.1841	-39.1155
D_20031116	-45.4762	-43.2796	-39.8207	-45.1653	-44.5918	-42.1253	-37.0543
D_20040404	-50.7555	-55.0668	-46.6104	-49.9457	-50.0917	-43.5745	-42.6703
D_20040718	-61.3526	-56.5421	-48.6281	-56.8499	-58.2721	-48.3261	-46.0637
D_20041031	-62.9554	-63.2275	-54.4632	-37.3851	-60.7992	-57.6635	-55.5473
D_20050320	-42.8527	-39.7297	-64.1379	-41.2551	-43.3736	-64.3849	-64.9542
D_20100627	-58.7610	-79.1065	-79.1605	-83.0820	-72.0546	-84.4598	-77.9355

All PS points in Fig. 4a do not correspond to buildings points. For identification of the building points the shape files generated through 'SARScape' were exported to 'ArcMap'. Building points were identified by overlaying the shape file of the PS points on the optical image of Mumbai (IRS-P6 Liss-4 image). The snapshot is shown in the Fig. 5a where the shape file was overlaid on the optical image. The area was zoomed in and the buildings points were identified. By clicking on the point the attributes values corresponding to that point were displayed on the window. One such building PS point and corresponding attribute is shown in Fig. 5b. This building point with latitude 18.9710 degrees and longitude 72.8072 degrees, showed the subsidence rate of 3.97 mm/year (low subsidence). The size of this identified building was found to be 33.61*19.31 m^2 (Fig. 6). The building was identified on Google Earth based on the latitude and longitude value and then size of the building was measured. Using this method, some building PS points were identified and deformation rate was estimated.

Time series plot of few building points identified using this method is shown in Fig.7. The legend shows the latitude and longitude of the corresponding PS point. It can be clearly seen from the figure that buildings corresponding to the points shown in the legend of Fig.7 are showing subsidence. Assuming the linear trend of the subsidence in the buildings, the linear equation and corresponding R^2 value is also shown in the figure. From the R^2 value, we can see that there is a good correlation between the linear trend and displacement trend shown by the buildings.

The probable cause of subsidence of the buildings in this area might be the hydrogeology of the area and lowering of the ground water table (Fig.8 & 9). Fig. 8 shows the hydrogeology map of the western part of the study area. From the map it is evident that the Worli-Colaba area comes under 'soft rock' category. Marine alluvium is found in the coastal area which is potential acquifer zone.

The ground water occurs under water table condition in sandy / gritty layers. The alluvial fill of low lying areas underlain by weathered basalt has ground water which can lead to the subsidence of the area. The pressure exerted by the buildings results in the development of tensional forces in overlying confining layer material. Consequently, compaction of overlying confining layer material takes place and land subsidence occurs.

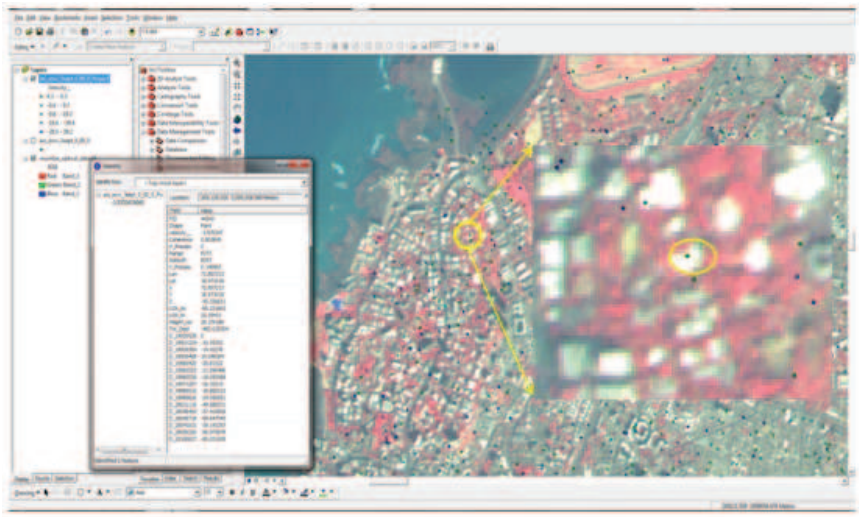

Figure 5a: Snapshot of the Building PS point identified by overlaying the shape file on the IRS-P6 Liss-4 image using ArcMAP software

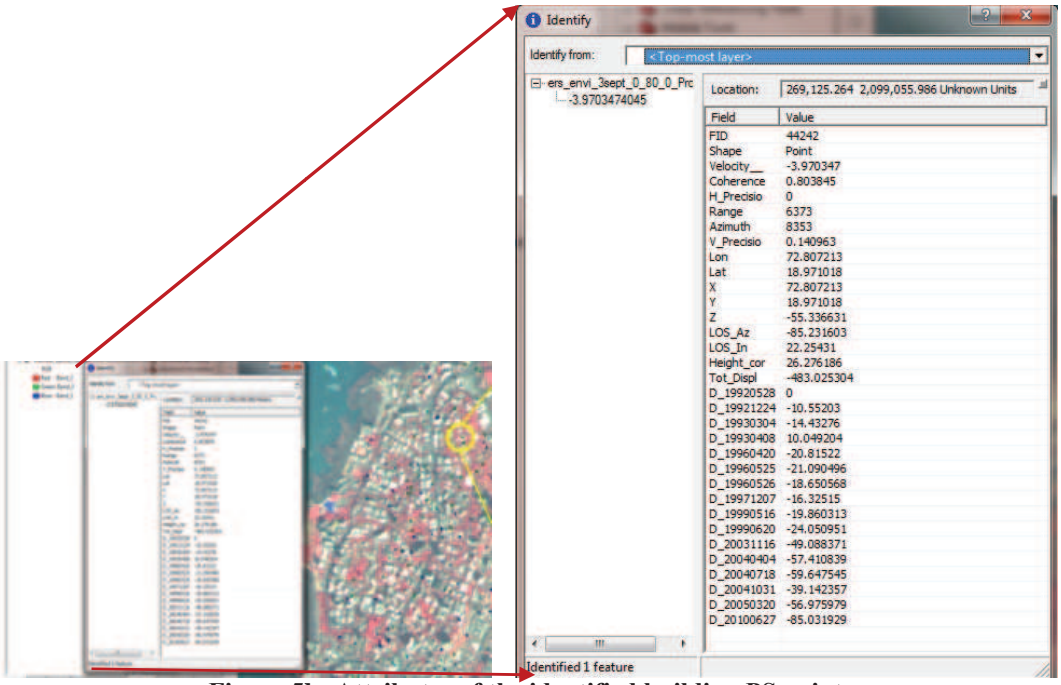

Figure 5b: Attributes of the identified building PS point

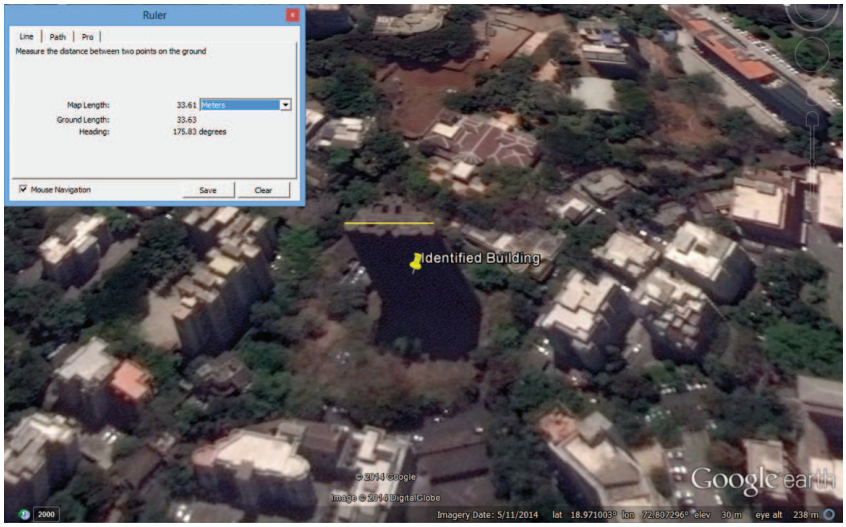

Figure 6: Snapshot of the building corresponding to the PS point identified on the Google Earth
(Image courtesy: googleearth.com)

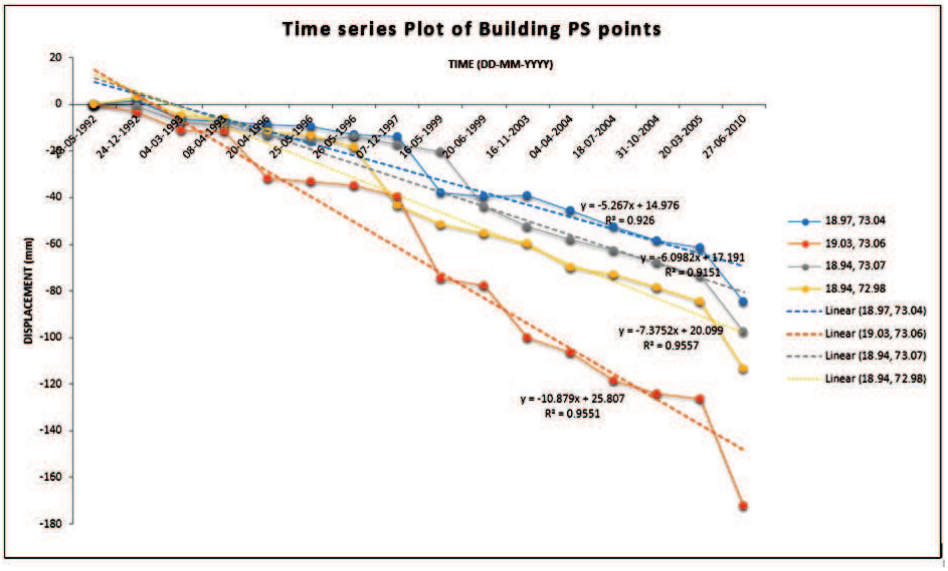

Figure 7: Time Series plot of few building PS points with legend showing latitude and longitude of the particular building PS point

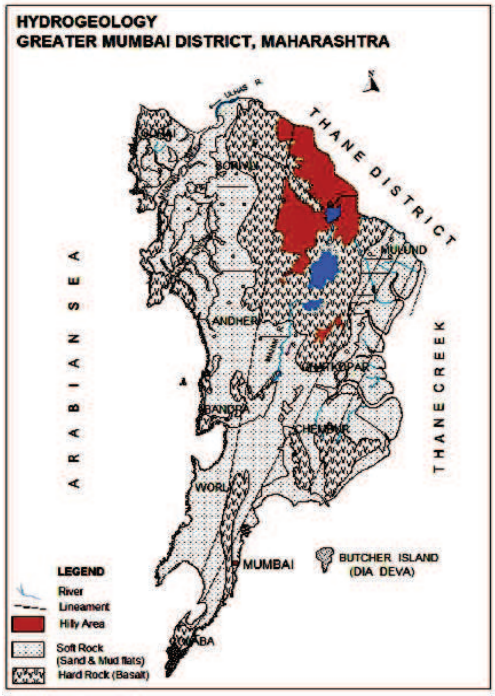

Source: CGWB report: 1618/DB/2009

Figure 8: Hydrogeology map of the western zone of the study area

The other reason that contributes to the subsidence in the area is the fall of ground water level. Trend of water levels for pre-monsoon and post-monsoon periods for last ten years (1998-2007) have been computed for 4 National Hydrograph Network Stations (NHNS) (CGWB Report No. 1618/DB/2009). Analysis of long term water level trend data indicates fall in water levels has been observed in all the 4 NHNS and it ranges between 0.11 (Church Gate) and 0.38 m/year (A.M.C. Colony). During post-monsoon period, rise in water level of 0.09 m/year has been recorded at only 1 NHNS located at Mahroli (Chembur), while at 3 NHNS fall in water level have been recorded and it ranges between 0.02 in Colaba (Dandi)) and 0.26 m/year in A.M.C. Colony. Thus in the western zone of the study area, both during pre-monsoon and post-monsoon seasons, declining water level trends, as shown in Fig.9, have been recorded which might contribute to the subsidence of the western part of the study area.

It was observed that not all buildings in the study area are undergoing subsidence; in some area uplift is also observed. Ascertaining the causes of the subsidence and uplift require additional building parameters like construction year, building material, foundation of the building. The validation of the subsidence values could not be done due to non-availability of the field data.

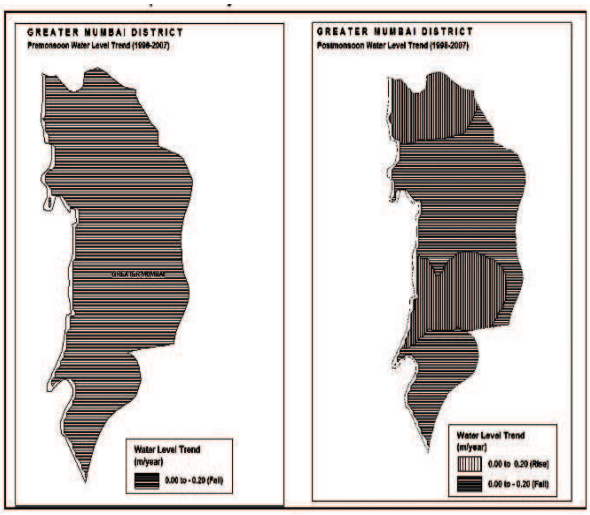

Source: CGWB report: 1618/DB/2009

Figure 9: Water level trend of the western zone of the study area

After identifying the endangered buildings, in future it is planned to study the selected building's parameters for analyzing the cause of the subsidence. The accuracy of the results can be improved by using more datasets. The density of PS points can be further

increased using high resolution X-band data which will help in decreasing the atmosphere related error. Use of high resolution TerraSAR-X data will improve the density of PS. As density is increased because of increasing the spatial resolution, more number of PS points will occur per square km which in turn will increase the number of PS points within 1.2 km which is the correlation length of atmosphere. More number of PS points within the correlation length of atmosphere will lead to elimination of the atmospheric phase. Two nearby PS points will have the same effect of atmosphere and hence the phase difference between these two points will eliminate the atmospheric phase and will help in improving the accuracy of the results obtained.

6. Conclusions

For the first time, building subsidence problem is addressed for Mumbai using PSInSAR technique. A methodology for the identification of the endangered building has been developed. The qualitative study shows that Mumbai city and surrounding areas are undergoing subsidence at the mean velocity of 5mm/year. The reason for the subsidence might be attributed to the hydrogeology of the area and the decreasing ground water level trend in the area. The accuracy of the results can be improved by using more datasets and use of high resolution TerraSAR-X data.

Acknowledgements

The authors are grateful to Shri A.S. Kiran Kumar, Director, Space Applications Centre (ISRO), Ahmedabad for his guidance and encouragement during the study. It is our immense pleasure to thank Dr. P.K. Pal, Deputy Director, EPSA, SAC, ISRO for his constant support. Thanks are also due to Dr. A.K. Shukla, Head, CVD for allowing to carry on this work. We are highly indebted to Dr. B.S. Gohil for his valuable suggestions on the manuscript. The authors also thank European Space agency (ESA) for providing ERS and ENVISAT data of Mumbai (project ID: 14600). Thanks are also due to SARMAP for providing evaluation version of SARScape software. We are also thankful to Mr. Chandrakant Ojha, Research Scholar, University of Rome, for providing useful feedbacks for improvement of the work. We also thank the anonymous reviewers for providing their critical comments which helped in improving the manuscript.

References

Beradino, P., G. Fornaro, R. Lanari and Sansosti (2002). A new algorithm for surface deformation monitoring based on small baseline differential SAR interferograms. IEEE Transactions on Geoscience and Remote Sensing, 40(11), 2375-2383.

Cascini, L., D. Peduto, D. Reale, L. Arena, S. Ferlisi, S. Verde and G. Fornaro (2013). Detection and monitoring of facilities exposed to subsidence phenomena via past and current generation SAR sensors. J. Geophys. Eng. 10, 064001 (14pp) doi:10.1088/1742-2132/10/6/064001.

CGWB Report No. 1618/DB/2009, *Sourabh Gupta*, Ground Water Information, Greater Mumbai District, Maharashtra, CGWB, Ministry of Water Resources, Central Region Nagpur , 2009.

Crosetto M., O. Monserrat, M. Cuevas-González, N. Devanthéry and B. Crippa (2013). Analysis of X-band very high resolution persistent scatterer interferometry data over urban areas. International Archives of the Photogrammetry, Remote Sensing and Spatial Information Sciences, Volume XL-1/W1, ISPRS Hannover Workshop 2013, 21 – 24 May 2013, Hannover, Germany, 47-51.

Crosetto, M., O. Monserrat, M. Cuevas-González, N. Devanthéry, G. Luzi, B. Crippa (2014). Measuring thermal expansion using X-band persistent scatterer interferometry. ISPRS Journal of Photogrammetry and Remote Sensing (*paper in press*).

Esfahany, S.S., (2008). Improving persistent scatterer interferometry results for deformation monitoring (Case study on the Gardanne mining site). M.Sc. Thesis, July 2008.

Ferretti, C. Prati and F. Rocca (2001). Permanent scatterers in SAR interferometry. IEEE Trans. on Geosc. and Rem. Sens., Vol. 39, No. 1, 8-20.

Ferretti, A., A. Fumagalli, F. Novali, C. Prati, F. Rocca and A. Rucci (2011). A new algorithm for processing interferometric data stacks: SqueeSAR, IEEE transactions on Geoscience and Remote Sensing, Vol. 49, No.9, 3460-70.

Kampes, B. and A. Nico (2005). The STUN algorithm for persistent scatterer interferometry. In: Proceedings of the FRINGE Workshop 2005, Frascatti, Italy, 28 November - 2 December: 16.1, 2005.

Karila, K., Mika Karjalainen, Juha Hyyppä, Jarkko Koskinen, Veikko Saaranen and Paavo Rouhiainen (2013). A Comparison of Precise Leveling and Persistent Scatterer SAR Interferometry for Building Subsidence Rate Measurement, ISPRS Int. J. Geo-Inf. 2013, 2, 797-816; doi:10.3390/ijgi2030797, 797-816.

Ketelaar, V.B.H. (2009). Satellite radar interferometry subsidence monitoring techniques. Delft University of technology, Netherlands. Springer Publication. ISBN: 978-1-4020-9427-9.

Yonghong, Z., H. Wu and X. Liu, (2014). Measuring subsidence of transport infrastructures with time series TerraSAR-X images. EUSAR Proceedings, 2014, E4.4, ISBN 978-3-8007-3607-2/ISSN 2197-4403, 850-853.